

# A High Spectral Efficiency Coherent Microwave Photonic Link Employing Both Amplitude and Phase Modulation With Digital Phase Noise Cancellation

Xiang Chen, *Student Member, IEEE*, and Jianping Yao, *Fellow, IEEE, Fellow, OSA*

**Abstract**—A high spectral efficiency coherent microwave photonic link (MPL) supporting amplitude and phase modulation incorporating a digital phase noise cancellation is proposed and experimentally demonstrated. At the transmitter, a continuous-wave light wave is amplitude- and phase-modulated by two microwave vector signals carried by a microwave carrier at an identical frequency. The modulated optical signal is polarization multiplexed with an unmodulated optical carrier and transmitted over a length of a single-mode fiber (SMF). At the receiver, the optical signal is detected coherently by a coherent receiver to which a local oscillator (LO) laser source is also applied. Through advanced digital signal processing, the microwave vector signals are recovered, and the phase noise introduced by both the transmitter laser source and LO laser source is cancelled. An experiment is performed. The transmission of a 2.5-Gb/s 16-QAM and a 1.25-Gb/s QPSK microwave vector signals both at 2.5 GHz over a 25-km SMF is implemented. The total bit rate of the MPL is 3.75 Gb/s. The transmission performance of the MPL in terms of error vector magnitudes and bit error rates is evaluated.

**Index Terms**—Digital signal processing (DSP), high spectral efficiency, laser phase noise, microwave photonic link (MPL), optical coherent detection, phase noise cancellation (PNC).

## I. INTRODUCTION

THE transmission of microwave signals over an optical fiber, or radio over fiber, is considered a potential solution for next generation broadband wireless access networks since a radio over fiber link or microwave photonic link (MPL) presents several advantages over a conventional copper coaxial analog link, including a much wider bandwidth, lower link loss, and immunity to electromagnetic interferences [1]–[3]. In a conventional MPL, intensity-modulation and direct-detection (IM/DD) is usually employed which has an advantage of implementation simplicity. However, compared with a coherent MPL which can detect both intensity- and phase-modulated signals, an MPL employing IM/DD has a much lower spectral efficiency, since direct detection can only detect an intensity-modulated signal. For broadband wireless access networks, high spectral

efficiency is always needed. In addition, a coherent MPL has a receive sensitivity of about 20 dB higher than that of an IM/DD MPL, which provides an added advantage to a coherent MPL [4].

Numerous solutions have been proposed to implement coherent MPLs recently [5]–[12]. In [5], [6], a phase-modulation and coherent-detection (PM/CD) MPL was proposed. The phase noise was cancelled through the use of a digital phase locked loop. In [7], [8], two intensity-modulation and coherent-detection (IM/CD) MPLs were proposed in which the phase noise was cancelled by digital signal processing (DSP)-based envelope detection or DSP-based coherent detection. The limitation of the schemes is that only the phase [5], [6] or amplitude [7], [8] information on the optical carrier can be detected, thus the spectral efficiency is still limited. To increase the spectral efficiency, in [9] we proposed a photonic approach to modulating two microwave vector signals, which have the same RF center frequency, on a single optical carrier employing optical IQ modulation and coherent detection. The spectral efficiency is significantly increased, but the phase noise introduced by the transmitter laser source was not cancelled, which will degrade the transmission performance. A simple way to avoid the phase noise from the local oscillator (LO) laser source is to use an additional fiber to deliver an LO signal from the transmitter to the receiver [10]–[12]. But the system cost is increased. In addition, because of the link loss, the LO signal needs to be amplified at the receiver by an optical amplifier to satisfy the power level needed for coherent detection, which may introduce an additional noise due to the amplified spontaneous emission noise from the optical amplifier.

In this paper, we propose and experimentally demonstrate a high spectral efficiency coherent MPL supporting amplitude and phase modulation with digital phase noise cancellation (PNC) without using an additional fiber link. At the transmitter, a light wave from a laser source is split into two channels. In the upper channel, the light wave is first intensity modulated by a 16 quadrature amplitude modulation (16-QAM) microwave vector signal and then phase modulated by a quadrature phase shift keying (QPSK) microwave vector signal. The light wave in the lower channel is not modulated. Then, the two light waves from the two channels are polarization multiplexed at the polarization beam splitter (PBS) and sent to a receiver over a single mode fiber (SMF). At the receiver, the two orthogonally polarized light waves are demultiplexed by a second PBS and then detected by a coherent optical receiver, to generate four currents which contain the information of the 16-QAM

Manuscript received December 15, 2014; revised March 5, 2015 and March 30, 2015; accepted March 31, 2015. Date of publication April 1, 2015; date of current version June 3, 2015. This work was supported by the Natural Sciences and Engineering Research Council of Canada.

The authors are with the Microwave Photonics Research Laboratory, School of Electrical Engineering and Computer Science, University of Ottawa, Ottawa ON K1N 6N5, Canada (e-mail: jpyao@eecs.uOttawa.ca).

Color versions of one or more of the figures in this paper are available online at <http://ieeexplore.ieee.org>.

Digital Object Identifier 10.1109/JLT.2015.2419456

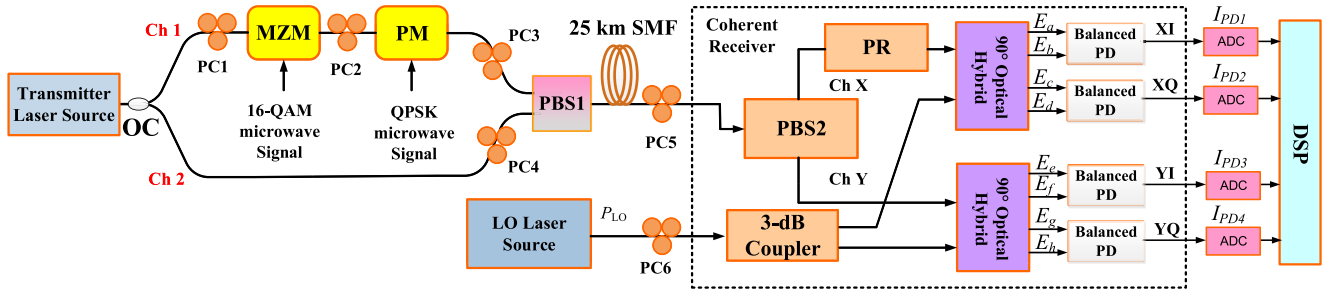


Fig. 1. Schematic of the proposed coherent MWP link with a DSP-based PNC module. ADC: analog-to-digital converter, OC: optical coupler, PC: polarization controller, CW laser: continuous-wave laser, balanced PD: balanced photodetector, MZM: Mach-Zehnder modulator, QPSK: quadrature phase shift keying, PM: phase modulator, PBS: polarization beam splitter, PR: polarization rotator, 16-QAM: 16 quadrature amplitude modulation, SMF: single mode fiber.

and QPSK signals. An algorithm is developed to recover the 16-QAM and the QPSK microwave vector signals while cancelling the phase noise introduced by both the transmitter laser source and LO laser source. The proposed technique is validated by an experiment. The transmission of a 2.5-Gb/s 16-QAM and a 1.25-Gb/s QPSK microwave vector signals over a 25-km SMF is demonstrated. The transmission performance is evaluated by measuring the error vector magnitudes (EVMS). The EVM of the recovered 16-QAM microwave vector signal can reach 8.05% and that of the recovered QPSK microwave vector signal can reach 8.23%. The bit error rates (BERs) calculated from the measured EVMS are also evaluated. Compared with coherent-detection MPLs based only on phase [5], [6], or amplitude modulation [7], [8], the spectral efficiency of the proposed scheme is significantly increased while maintaining the same transmission performance.

## II. PRINCIPLE OF OPERATION

Fig. 1 shows the schematic diagram of the proposed high spectral efficiency coherent MPL. At the transmitter, a light wave from a CW laser source is split by an optical coupler (OC) (95% and 5% optical powers for Channel 1 and Channel 2, respectively) into two channels. In Channel 1, the light wave is amplitude- and phase-modulated by a 16-QAM and a QPSK microwave vector signal, respectively, at a chirp-free single-electrode Mach-Zehnder modulator (MZM) and a phase modulator (PM) while the light wave in Channel 2 is not modulated. The two light waves from the two channels are then polarization multiplexed at a PBS (PBS1) and sent to a receiver via a 25-km SMF. At the receiver, a second PBS (PBS2) which is incorporated in the polarization- and phase-diversity coherent optical receiver (Discovery Semiconductors DP-QPSK 40/100 Gb/s Coherent Receiver) is used to demultiplex the two orthogonally polarized light waves (Channel X and Channel Y), which are then sent to two 90° optical hybrids inside the coherent optical receiver. An LO signal from a second laser source is split into two channels and also sent to the two hybrids. After balanced detection in the coherent optical receiver, four channels (XI, XQ, YI and YQ) of signals corresponding to the in-phase and quadrature (IQ) components of the two orthogonally polarized signals from the PBS2 are obtained, which are then sent to a DSP-based PNC module. An algorithm is developed to recover the 16-QAM microwave vector signal and the QPSK

microwave vector signal while cancelling the phase noise introduced by both the transmitter and LO laser sources.

At the transmitter, for Channel 1, the MZM is biased at the quadrature point and 16-QAM microwave vector signal is applied to the MZM via the RF port. The optical field at the output of the MZM is given by

$$E_0(t) = \sqrt{2P_{s1}L_{s1}} \cos \left[ \frac{\pi S_{RF-16QAM}(t)}{2V_{\pi IM}} + \frac{\pi}{4} \right] \times \exp \{ j[\omega_c t + \varphi_{c1}(t)] \} \quad (1)$$

where  $P_{s1}$  is the optical power at the input of Channel 1,  $\omega_c$  is the angular frequency of the light wave,  $S_{RF-16QAM}(t)$  is the microwave vector signal applied to the MZM, the modulation format is 16-QAM,  $\varphi_{c1}(t)$  is the phase term of the transmitter laser source for Channel 1,  $V_{\pi IM}$  is the half-wave voltage of the MZM, and  $L_{s1}$  is the link loss between the OC and PBS1 for Channel 1.

Then, the amplitude-modulated optical signal is phase-modulated by a QPSK microwave vector signal. The optical field at the output of the PM is given by

$$E_1(t) = \sqrt{2P_{s1}L_{s1}} \cos \left[ \frac{\pi S_{RF-16QAM}(t)}{2V_{\pi IM}} + \frac{\pi}{4} \right] \times \exp \left\{ j \left[ \omega_c t + \varphi_{c1}(t) + \frac{\pi S_{RF-QPSK}(t)}{V_{\pi PM}} \right] \right\} \quad (2)$$

where  $S_{RF-QPSK}(t)$  is the QPSK microwave vector signal applied to the PM, the modulation format is QPSK and  $V_{\pi PM}$  is the half-wave voltage of the PM.

For Channel 2, the light wave is not modulated. The optical field at the output of Channel 2 is given by

$$E_2(t) = \sqrt{2P_{s2}L_{s2}} \exp \{ j[\omega_c t + \varphi_{c2}(t)] \} \quad (3)$$

where  $P_{s2}$  is the optical power at the input of Channel 2,  $\varphi_{c2}(t)$  is the phase term of the transmitter laser source for Channel 2, and  $L_{s2}$  is the link loss between the OC and PBS1 for Channel 2. Note,  $\varphi_{c1}(t)$  and  $\varphi_{c2}(t)$  are different, since the optical signals from the transmitter laser source are split by an OC and transmitted through two fibers.

Then, the two light waves from the two channels are polarization multiplexed at PBS1 and transmitted over the SMF. At the receiver, the two orthogonally polarized light waves are demultiplexed by PBS2 into two channels (Channel X and Channel Y).

The optical fields at the outputs of PBS2 for Channel X and Channel Y are given by

$$E_x(t) = E_1(t) \quad (4)$$

$$E_y(t) = E_2(t). \quad (5)$$

On the other hand, the optical field at the output of the LO laser source can be written as

$$E_{LO}(t) = \sqrt{2P_{LO}} \exp \{j [\omega_{LO}t + \varphi_{LO}(t)]\}. \quad (6)$$

Through tuning PC6, with the help of the polarization rotator in Fig. 1, the light wave from the LO laser source is co-polarized with the other optical signals at the inputs of the two 90° optical hybrids. At the outputs of the two 90° optical hybrids, eight optical fields are obtained, given by

$$\begin{aligned} & \begin{bmatrix} E_a(t) & E_b(t) & E_c(t) & E_d(t) \\ E_e(t) & E_f(t) & E_g(t) & E_h(t) \end{bmatrix} \\ &= \sqrt{L_h} \begin{bmatrix} \sqrt{L_f} E_x(t) & E_{LO}(t) e^{j\varphi_x} / \sqrt{2} \\ \sqrt{L_f} E_y(t) & E_{LO}(t) e^{j\varphi_y} / \sqrt{2} \end{bmatrix} \\ & \cdot \begin{pmatrix} 1 & 1 & 1 & 1 \\ 1 & e^{j\pi} & e^{j\pi/2} & e^{-j\pi/2} \end{pmatrix} \end{aligned} \quad (7)$$

where  $L_h$  is the link loss caused by the two 90° optical hybrids,  $L_f$  is the link loss caused by the SMF, and  $\varphi_x, \varphi_y$  are the phase terms arising from the polarization mismatch between the signal and the light wave from the LO laser source.

By applying  $(E_a, E_b)$ ,  $(E_c, E_d)$ ,  $(E_e, E_f)$ ,  $(E_g, E_h)$  to four balanced PDs which are terminated with 50-Ω resistors, four output photocurrents are obtained, which are given by

$$\begin{aligned} I_{PD1} &= 2RL_h \sqrt{2P_{s1} P_{LO} L_f L_{s1}} \\ & \times \cos \left[ \pi S_{RF-16QAM}(t) / 2V_{\pi IM} + \frac{\pi}{4} \right] \\ & \times \cos [\Delta\omega t + \varphi_1(t) - \varphi_x + \pi S_{RF-QPSK}(t) / V_{\pi PM}] \end{aligned} \quad (8)$$

$$\begin{aligned} I_{PD2} &= 2RL_h \sqrt{2P_{s1} P_{LO} L_f L_{s1}} \\ & \times \cos \left[ \pi S_{RF-16QAM}(t) / 2V_{\pi IM} + \frac{\pi}{4} \right] \\ & \times \sin [\Delta\omega t + \varphi_1(t) - \varphi_x + \pi S_{RF-QPSK}(t) / V_{\pi PM}] \end{aligned} \quad (9)$$

$$I_{PD3} = 2RL_h \sqrt{2P_{s2} P_{LO} L_f L_{s2}} \cos [\Delta\omega t + \varphi_2(t) - \varphi_y] \quad (10)$$

$$I_{PD4} = 2RL_h \sqrt{2P_{s2} P_{LO} L_f L_{s2}} \sin [\Delta\omega t + \varphi_2(t) - \varphi_y] \quad (11)$$

with

$$\Delta\omega = \omega_c - \omega_{LO},$$

$$\varphi_1(t) = \varphi_{c1}(t) - \varphi_{LO}(t), \quad \varphi_2(t) = \varphi_{c2}(t) - \varphi_{LO}(t)$$

where  $\Delta\omega$  is the frequency difference between the transmitter laser source and the LO laser source,  $\varphi_1(t)$ ,  $\varphi_2(t)$  are the phase noise introduced by the transmitter laser source and the LO laser source. Before we explain the method to recover the 16-QAM microwave vector signal and the QPSK microwave vector

signal, it is important to investigate how the phase noise affects the 16-QAM microwave vector signal and the QPSK microwave vector signal.

First, an ideal situation is considered, where  $\Delta\omega = 0$  and no signal is sent to the PM ( $S_{RF-QPSK}(t) = 0$ ). Then, (8) can be rewritten as

$$\begin{aligned} I_{PD1} &= 2RL_h \sqrt{2P_{s1} P_{LO} L_f L_{s1}} \\ & \times \cos [\pi S_{RF-16QAM}(t) / 2V_{\pi IM} + \pi/4] \\ & \times \cos [\varphi_1(t) - \varphi_x]. \end{aligned} \quad (12)$$

From (12), it can be seen that the phase noise  $\varphi_1(t)$  is converted to an amplitude noise given by  $\cos(\varphi_1(t) - \varphi_x)$  at the output of the coherent receiver.

If  $\Delta\omega = 0$  and no signal is sent to the MZM, (8) can be expressed as

$$\begin{aligned} I_{PD1} &= 2RL_h \sqrt{2P_{s1} P_{LO} L_f L_{s1}} \cos(\pi/4) \\ & \times \left\{ \begin{aligned} & \cos[\varphi_1(t) - \varphi_x] \cos[\pi S_{RF-QPSK}(t) / V_{\pi PM}] \\ & - \sin[\varphi_1(t) - \varphi_x] \sin[\pi S_{RF-QPSK}(t) / V_{\pi PM}] \end{aligned} \right\}. \end{aligned} \quad (13)$$

As can be seen, the phase noise  $\varphi_1(t)$  is also converted to an amplitude noise given by  $\sin(\varphi_1(t) - \varphi_x)$ .

Then, a more realistic situation is considered where  $\Delta\omega \neq 0$  and both the intensity and phase of the optical light are modulated. Equations (8) and (9) can be further expanded as

$$\begin{aligned} I_{PD1} &= 2RL_h \sqrt{2P_{s1} P_{LO} L_f L_{s1}} \\ & \times [(A \times C - A \times D) - (B \times C - B \times D)] \quad (14) \\ I_{PD2} &= 2RL_h \sqrt{2P_{s1} P_{LO} L_f L_{s1}} \\ & \times [(A \times E + A \times F) - (B \times E + B \times F)] \quad (15) \end{aligned}$$

with

$$A = \cos [\pi S_{RF-16QAM}(t) / 2V_{\pi IM}] \cos(\pi/4)$$

$$B = \sin [\pi S_{RF-16QAM}(t) / 2V_{\pi IM}] \sin(\pi/4)$$

$$C = \cos [\Delta\omega t + \varphi_1(t) - \varphi_x] \cos [\pi S_{RF-QPSK}(t) / V_{\pi PM}]$$

$$D = \sin [\Delta\omega t + \varphi_1(t) - \varphi_x] \sin [\pi S_{RF-QPSK}(t) / V_{\pi PM}]$$

$$E = \cos [\Delta\omega t + \varphi_1(t) - \varphi_x] \sin [\pi S_{RF-QPSK}(t) / V_{\pi PM}]$$

$$F = \sin [\Delta\omega t + \varphi_1(t) - \varphi_x] \cos [\pi S_{RF-QPSK}(t) / V_{\pi PM}].$$

In (14) and (15), if we assume that both the QPSK and the 16-QAM microwave vector signals are small signals, then  $A \times D$  and  $A \times E$  represent the detected QPSK microwave vector signals at the outputs of the coherent receiver ( $I_{PD1}$  and  $I_{PD2}$ ). The frequencies of the detected QPSK microwave vector signals are up converted because of the frequency difference between the transmitter laser source and LO laser source. And  $B \times C$ ,  $B \times F$  represent the detected 16-QAM microwave vector signals and their frequencies are also up converted due to the same reason. If the center frequencies and bandwidths of the QPSK microwave vector signal and the 16-QAM microwave vector signal are

identical, for each output of the coherent receiver ( $I_{PD1}$  and  $I_{PD2}$ ), the spectra of the detected 16-QAM signal and the detected QPSK signal are completely overlapped. In addition, both the detected QPSK and 16-QAM microwave vector signals are affected by the phase noise introduced by both the transmitter laser source and LO laser source. Apparently, it is impossible to recover and demodulate the two microwave vector signals directly from the outputs of the coherent receiver. To demodulate the 16-QAM microwave vector signal and the QPSK microwave vector signal, DSP algorithms are employed to cancel the phase noise, eliminate the frequency shift and recover the signals from the overlapped spectra.

First, the four signals,  $I_{PD1}$ ,  $I_{PD2}$ ,  $I_{PD3}$  and  $I_{PD4}$  are separately sampled and digitized by four ADCs. Then, the DSP algorithm is employed [8]. By summing the squared magnitudes of  $I_{PD1}$  and  $I_{PD2}$ , we can obtain

$$\begin{aligned} I_1 &= I_{PD1}^2 + I_{PD2}^2 \\ &= 4R^2 L_h^2 L_f P_{s1} P_{LO} L_{s1} \\ &\quad \times \{1 - \sin[\pi S_{RF-16QAM}(t)/V_{\pi IM}]\} \\ &\approx 4R^2 L_h^2 L_f P_{s1} P_{LO} L_{s1} \{1 - [\pi S_{RF-16QAM}(t)/V_{\pi IM}]\}. \end{aligned} \quad (16)$$

As can be seen, the QPSK microwave vector signal is not present in the expression and the phase noise is cancelled, thus a recovery of the 16-QAM microwave vector signal free from phase noise is realized.

Also, through DSP, we can obtain (17) as shown at the bottom of the page.

In (17), the maximum frequency of  $\varphi(t)$  is determined by the linewidth of the transmitter laser source. So, if the lower frequency of the QPSK microwave vector signal is higher than the maximum frequency of  $\varphi(t)$ , the QPSK microwave vector signal can be simply selected by a digital bandpass filter. The signal at the output of the digital band-pass filter is then expressed as

$$I_2 \approx \frac{\pi S_{RF-QPSK}(t)}{V_{\pi PM}}. \quad (18)$$

Similarly, the 16-QAM microwave vector signal is not present in the expression and the phase noise is cancelled, thus a recovery of the QPSK microwave vector signal free from phase noise is also realized.

### III. EXPERIMENTAL DETAILS

An experiment based on the setup shown in Fig. 1 is performed. A tunable laser source (TLS) operating at 1550.57 nm with a linewidth of about 100 kHz and an output power of 16 dBm is utilized as the transmitter laser source. The light wave from the TLS is split into two channels by an OC with a splitting ratio of 95:5 (95% optical power for Channel 1 and 5% optical power for Channel 2). In Channel 1, the light wave is sent via a polarization controller (PC1) to a chirp-free single-electrode MZM (JDS-Uniphase) that is biased at the quadrature point, and is modulated by a 16-QAM microwave vector signal. Then, the amplitude-modulated light wave is sent to a PM (JDS-Uniphase) via a second PC (PC2), and is phase-modulated by a QPSK microwave vector signal. The optical signal at the output of the PM is then sent to PBS1 via PC3. The polarization extinction ratio of PBS1 is 20 dB. Both the 16-QAM microwave vector signal and the QPSK microwave vector signal are generated by an arbitrary waveform generator (Tektronix AWG7102) with a carrier frequency at 2.5 GHz. The symbol rate for each of the digital modulated microwave signals is 625 MSymbol/s, or the bit rate for the 16-QAM microwave vector signal is 2.5 Gb/s and for the QPSK microwave vector signal is 1.25 Gb/s, and the total bit rate for the whole system is 3.75 Gb/s. The MZM has a bandwidth of 10 GHz, a half-wave voltage of about 5.5 V and an insertion loss of 4.5 dB, and the PM has a bandwidth of 20 GHz, a half-wave voltage of 5 V and an insertion loss of 4.5 dB.

In Channel 2, the light wave is not modulated, which is sent to PBS1 via PC4. PC3 and PC4 are used to make the polarization directions of the two signals align with the two principal axes of PBS1, thus the two light waves are polarization multiplexed, which are transmitted over a 25-km SMF and sent to a coherent receiver (Discovery Semiconductors DP-QPSK 40/100 Gb/s Coherent Receiver Lab Buddy) via PC5. Through tuning PC5, the two polarization multiplexed light waves can be demultiplexed by PBS2, which is inside the coherent receiver (Here, PC5 can be replaced by a dynamic polarization controller in a practical system [13]). On the other hand, a second TLS (Yokogawa AQ2201) operating at 1550.619 nm with a linewidth of about 1 MHz and an output power of 9.3 dBm is used as the LO laser source. The wavelength difference between the transmitter laser source and the LO laser source is 0.048 nm, corresponding to a beat frequency of about 6 GHz. The light wave from the LO laser source is sent to the LO port of the coherent receiver through PC6. A Digital Storage Oscilloscope (Agilent DSO-X

$$\begin{aligned} I_2 &= \text{atan} \left[ \frac{(I_{PD2} \times I_{PD3} - I_{PD1} \times I_{PD4})}{(I_{PD1} \times I_{PD3} + I_{PD2} \times I_{PD4})} \right] \\ &= \text{atan} \left\{ \frac{\sin[\pi S_{RF-QPSK}(t)/V_{\pi PM} + \varphi_{c1}(t) - \varphi_{c2}(t) - \varphi_x + \varphi_y]}{\cos[\pi S_{RF-QPSK}(t)/V_{\pi PM} + \varphi_{c1}(t) - \varphi_{c2}(t) - \varphi_x + \varphi_y]} \right\} \\ &= \pi S_{RF-QPSK}(t)/V_{\pi PM} + \varphi(t) \end{aligned} \quad (17)$$

with

$$\varphi(t) = \varphi_{c1}(t) - \varphi_{c2}(t) - \varphi_x + \varphi_y.$$

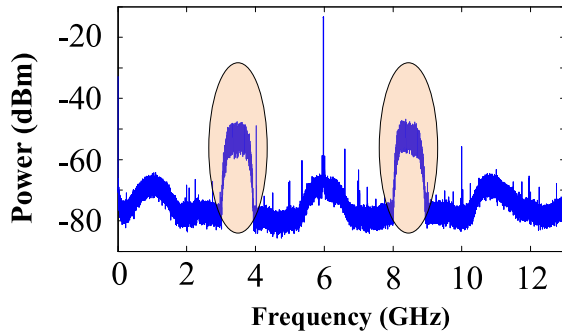


Fig. 2. Spectrum of the signals at the first output port of the coherent receiver ( $I_{PD1}$ ).

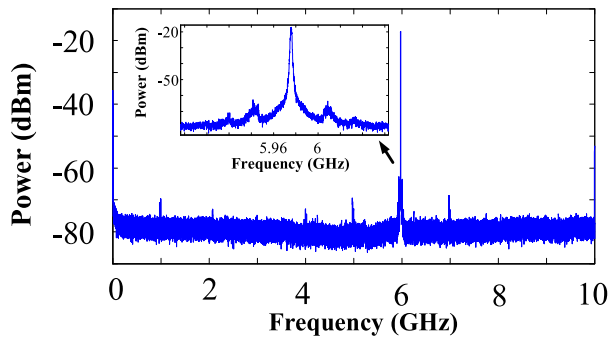


Fig. 3. Spectrum of the signal at the third output port of the coherent receiver ( $I_{PD3}$ ).

93204A) is employed to perform the analog-to-digital conversion at a sampling rate of 40 GSa/s. The sampled signals ( $I_{PD1}$ ,  $I_{PD2}$ ,  $I_{PD3}$  and  $I_{PD4}$ ) are processed off-line in a computer with the proposed DSP algorithms developed to recover the 16-QAM and the QPSK microwave vector signals while cancelling the phase noises from the transmitter and LO laser sources.

In order to recover the 16-QAM and the QPSK microwave vector signals free from the phase noise, the lengths of the four paths for the in-phase and the quadrature components of the two orthogonally polarized signals from PBS2 should be precisely matched. In the experiment, the length differences of the cables at the outputs of the coherent receiver between the four paths are controlled within 1 mm, and the four paths inside the coherent receiver are well matched. Thus, the proposed DSP-based PNC algorithm is applicable for a coherent system using any commercial laser sources that are designed for optical communications applications.

Fig. 2 shows the spectrum at the first output port of the coherent receiver ( $I_{PD1}$ ), which contains the 16-QAM and the QPSK microwave vector signals. As can be seen, the detected microwave vector signals (the signals with the center frequencies of 3.5 and 8.5 GHz) in Fig. 2 are just the mixing products of the 2.5-GHz transmitted microwave vector signals and the 6-GHz electrical carrier whose frequency is just the frequency difference between the two laser sources. In addition, the spectra of the 16-QAM microwave vector signal and QPSK microwave vector signal are completely overlapped, as mentioned in Section II.

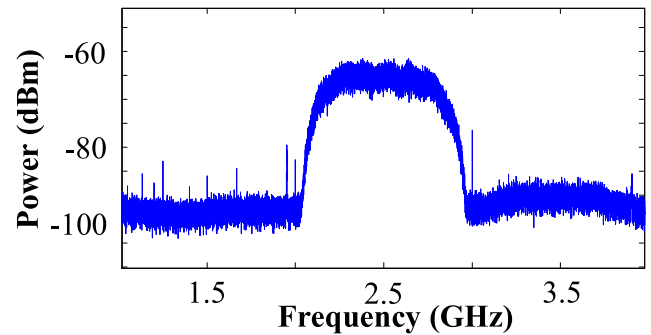


Fig. 4. Spectrum of the recovered 16-QAM microwave vector signal at the output of the DSP-based PNC module.

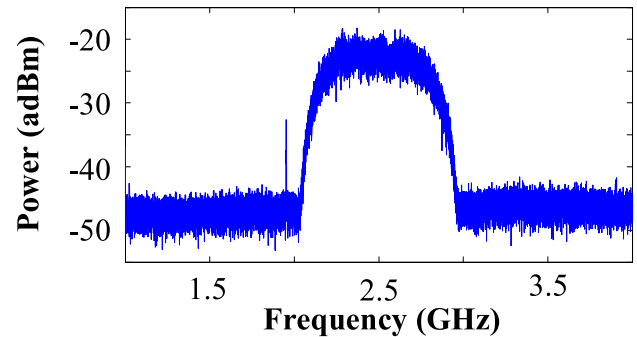


Fig. 5. Spectrum of the recovered QPSK microwave vector signal at the output of the DSP-based PNC module.

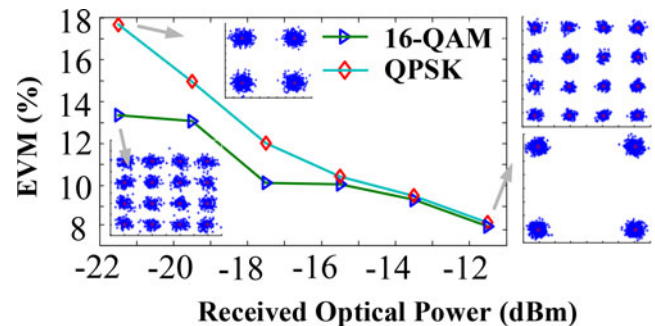


Fig. 6. EVM measurements at different received optical power levels for the QPSK and the 16-QAM signal transmitted over the 25-km SMF.

Fig. 3 shows the spectrum at the third output port of the coherent receiver ( $I_{PD3}$ ). As can be seen, the microwave vector signals contains a strong phase noise which is introduced from both the transmitter laser source and LO laser source. Figs. 4 and 5 show the spectra of the recovered 16-QAM and QPSK microwave vector signals at the output of the DSP-based PNC module. Apparently, the signals are frequency translated back to the exact radio frequencies of the original signals after the digital signal processing.

Then, we evaluate the performance of the system in terms of EVMs for the recovered microwave vector signals as a function of the received optical power. The results are shown in Fig. 6. As can be seen when the received optical power is  $-21.5$  dBm, the constellations of the 16-QAM microwave vector signal and the QPSK microwave vector signal are clear and well separated. In order to demonstrate the effectiveness of the proposed PNC

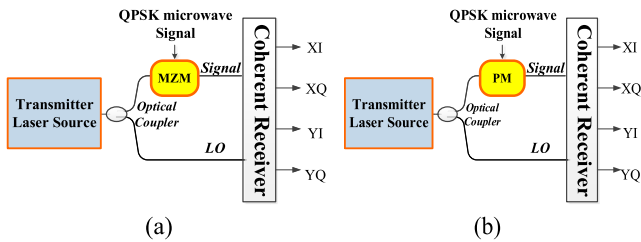


Fig. 7. Schematic diagrams of (a) an IM/CD MPL, and (b) a PM/CD MPL without digital PNC module.

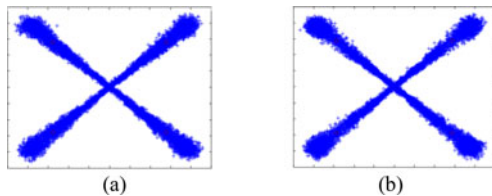


Fig. 8. Constellations of the detected QPSK microwave vector signal. (a) The IM/CD MPL without digital PNC module, (b) the PM/CD MPL without digital PNC module.

technique, we also measure the constellations of the detected signals for an IM/CD MPL and a PM/CD MPL without a digital PNC module. The experiment setups are shown in Fig. 7(a) and (b). Here, the microwave vector signal for both setups is a QPSK signal with a center frequency of 2.5 GHz and a symbol rate of 625 MSymbol/s. The linewidth of the laser source is 100 KHz. As discussed in Section II, the output signals at XI ports of the coherent receivers in Fig. 7(a) and (b) can be expressed as (12) and (13). Fig. 8(a) and (b) shows the constellations of the output signals at the XI ports of the coherent receivers in Fig. 7(a) and (b). As can be seen, the quality of the recovered QPSK microwave vector signals are very poor which confirms that the QPSK microwave vector signals for both cases are strongly affected by the phase noise.

Finally, we evaluate the BER performance of the system. Assuming that the noise after the digital PNC module is a stationary random process with Gaussian statistics, we can calculate the BERs of  $M$ -ary QAM from the EVMs based on the relationship given by

$$\bar{P}_{M-QAM} = \frac{2}{\log_2 M} \left( 1 - \frac{1}{\sqrt{M}} \right) \times \text{erfc} \left( \sqrt{\frac{3}{2(M-1)} \times SNR} \right) \quad (19)$$

with

$$SNR = 1/EVM^2 \quad (20)$$

where  $\text{erfc}()$  is the complementary error function and SNR is the signal-to-noise ratio [14]–[17]. The BERs as a function of the received optical power calculated from the measured EVMs are shown in Fig. 9. Again, when the received optical power is  $-21.5$  dBm, the BER is  $10^{-8}$  for the QPSK signal, which is sufficiently small to recover the original signal. The BER for the 16-QAM signal is  $10^{-4}$ , which is poorer than that of the QPSK signal. By using a state-of-the-art forward error correction (FEC) technique, the recovered signal would have a signal

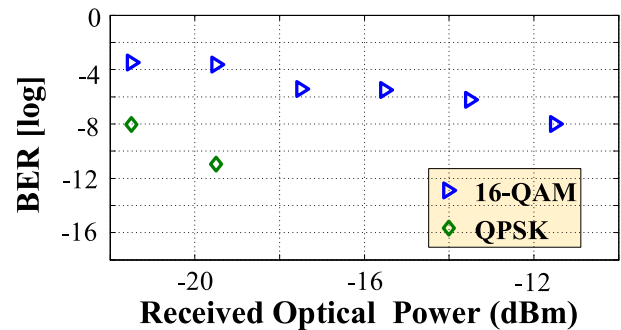


Fig. 9. BERs at different received optical power levels for the QPSK and the 16-QAM microwave vector signals transmitted over 25-km SMF.

quality that is still suitable for error-free transmission [6], [18], [19]. When the received optical power is  $-13.5$  dBm, according to (19), the estimated signal-to-noise ratios of the QPSK and 16-QAM microwave vector signals after the PNC module are 20.45 and 20.61 dB, respectively. For such signal-to-noise ratios, error-free detection with higher-order modulation formats can be achieved by using the FEC techniques. Considering the FEC limit (The FEC technique can be applied to improve a raw BER of up to  $3 \times 10^{-3}$  to an effective BER of  $1 \times 10^{-15}$ , at the expense of a 6.7% overhead [19]), for a signal with a signal-to-noise ratio of 20.45 dB, the highest-order modulation format for error-free detection is 32-QAM. So the spectrum efficiency of the proposed scheme can reach 10 bit/s/Hz. For the conventional IM/DD MPL in [7], when the received optical power was  $-12.5$  dBm, since the SNR and the estimated BER of the received microwave vector signal were 9.3299 dB and  $3 \times 10^{-3}$ , the highest-order modulation format for error-free detection is QPSK. So the spectral efficiency is only 2 bit/s/Hz.

#### IV. CONCLUSION

A high spectral efficiency coherent MPL supporting simultaneous amplitude and phase modulation with digital phase noise cancellation was proposed and experimentally demonstrated. Through advanced DSP, amplitude- and phase-modulated microwave vector signals could be recovered and the phase noise introduced by both the transmitter laser source and LO laser source could be effectively cancelled. The proposed technique was evaluated experimentally. Two microwave vector signals with one being a 16-QAM microwave vector signal at 2.5 Gb/s and another being a QPSK microwave vector signal at 1.25 Gb/s were transmitted over a 25-km SMF link and recovered at the receiver. The EVMs for the recovered 16-QAM and QPSK microwave vector signals were measured to be 8.05% and 8.23%, respectively, which are good enough to achieve error-free transmission with FEC.

#### REFERENCES

- [1] A. J. Seeds, "Microwave photonics," *IEEE Trans. Microw. Theory Tech.*, vol. 50, no. 3, pp. 877–887, Mar. 2002.
- [2] J. P. Yao, "Microwave photonics," *J. Lightw. Technol.*, vol. 27, no. 3, pp. 314–335, Feb. 2009.
- [3] J. Capmany and D. Novak, "Microwave photonics combines two worlds," *Nature Photon.*, vol. 1, no. 6, pp. 319–330, Jun. 2007.
- [4] G. P. Agrawal, *Fiber-Optic Communication Systems*, 3rd ed. Hoboken, NJ, USA: Wiley, 2002, pp. 478–479.

- [5] A. Caballero, D. Zibar, and I. T. Monroy, "Performance evaluation of digital coherent receivers for phase-modulated radio-over-fiber links," *J. Lightw. Technol.*, vol. 29, no. 21, pp. 3282–3292, Nov. 2011.
- [6] A. Caballero, D. Zibar, and I. T. Monroy, "Digital coherent detection of multi-gigabit 40 GHz carrier frequency radio-over-fiber signals using photonic down conversion," *Electron. Lett.*, vol. 46, no. 1, pp. 57–58, Jan. 2010.
- [7] X. Chen, T. Shao, and J. P. Yao, "Digital phase noise cancellation for a coherent-detection microwave photonic link," *IEEE Photon. Technol. Lett.*, vol. 26, no. 8, pp. 805–808, Apr. 2014.
- [8] X. Chen and J. P. Yao, "A coherent microwave photonic link with digital phase noise cancellation," in *Proc. IEEE Int. Top. Meet. Microw. Photon. Conf.*, Oct. 2014, pp. 438–441.
- [9] Y. Chen, T. Shao, A. Wen, and J. P. Yao, "Microwave vector signals transmission over an optical fiber based on IQ modulation and coherent detection," *Opt. Lett.*, vol. 39, no. 6, pp. 1509–1512, Mar. 2014.
- [10] Y. Pei, J. P. Yao, K. Xu, J. Li, Y. Dai, and J. Lin, "Advanced DSP technique for dynamic range improvement of a phase-modulation and coherent-detection microwave photonic link," in *Proc. IEEE Int. Top. Meet. Microw. Photon. Conf.*, Oct. 2013, pp. 72–75.
- [11] T. R. Clark and M. L. Dennis, "Coherent optical phase-modulation link," *IEEE Photon. Technol. Lett.*, vol. 19, no. 16, pp. 1206–1208, Aug. 2007.
- [12] T. R. Clark, S. R. O'Connor, and M. L. Dennis, "A phase-modulation IQ-demodulation microwave-to-digital photonic link," *IEEE Trans. Microw. Theory Technol.*, vol. 58, no. 11, pp. 3069–3058, Nov. 2010.
- [13] X. S. Yao, L.-S. Yan, B. Zhang, A. E. Willner, and J. Jiang, "All-optic scheme for automatic polarization division demultiplexing," *Opt. Exp.*, vol. 15, no. 12, pp. 7407–7414, Jun. 2007.
- [14] D. H. Wolaver, "Measure error rates quickly and accurately," *Electron. Des.*, vol. 43, no. 11, pp. 89–98, May. 1995.
- [15] A. Brillant, *Digital and Analog Fiber Optic Communication for CATV and FTTx Applications*. Bellingham, WA, USA: SPIE, 2008, pp. 653–660.
- [16] V. J. Urick, J. X. Qiu, and F. Bucholtz, "Wide-band QAM-over-fiber using phase modulation and interferometric demodulation," *IEEE Photon. Technol. Lett.*, vol. 16, no. 10, pp. 2374–2376, Oct. 2004.
- [17] G. P. Agrawal, *Fiber-Optic Communication Systems*, 4th ed. Hoboken, NJ, USA: Wiley, 2010, pp. 151–157.
- [18] G. Hill, *The Cable and Telecommunications Professionals' Reference: Transport Networks*, vol. 3. Burlington, MA, USA: Focal Press, 2008, pp. 203–206.
- [19] R. Schmogrow, D. Hillerkuss, S. Wolf, B. Bäuerle, M. Winter, P. Kleinow, B. Nebendahl, T. Dippon, P. C. Schindler, C. Koos, W. Freude, and J. Leuthold, "512QAM Nyquist sinc-pulse transmission at 54 Gbit/s in an optical bandwidth of 3 GHz," *Opt. Exp.*, vol. 20, no. 6, pp. 6439–6447, Mar. 2012.

**Xiang Chen** (S'13) received the B.Eng. degree in communications engineering from the Donghua University, Shanghai, China, in 2009, and the M.Sc. degree in communications and information engineering from Shanghai University, Shanghai, in 2012. He is currently working toward the Ph.D. degree in electrical and computer engineering at the Microwave Photonics Research Laboratory, School of Electrical Engineering and Computer Science, University of Ottawa, Ottawa, ON, Canada.

His current research interests include coherent radio-over-fiber systems and the dynamic range of analog optical links.

**Jianping Yao** (M'99–SM'01–F'12) received the Ph.D. degree in electrical engineering from the Université de Toulon, Toulon, France, in December 1997.

In 1998, he joined the School of Electrical and Electronic Engineering, Nanyang Technological University, Singapore, as an Assistant Professor. In December 2001, he joined the School of Electrical Engineering and Computer Science, University of Ottawa, Ottawa, ON, Canada, as an Assistant Professor, where he became an Associate Professor in 2003, and a Full Professor in 2006. In 2007, he was appointed the University Research Chair in Microwave Photonics. From July 2007 to June 2010, he was the Director of the Ottawa-Carleton Institute for Electrical and Computer Engineering, where he was reappointed the Director in 2013. He is currently a Professor and University Research Chair with the School of Electrical Engineering and Computer Science, University of Ottawa. He has published more than 470 papers, including more than 270 papers in peer-reviewed journals and 200 papers in conference proceedings.

Dr. Yao is a Registered Professional Engineer of Ontario. He is a Fellow of the Optical Society of America and the Canadian Academy of Engineering. He is an IEEE MTT-S Distinguished Microwave Lecturer for 2013–2015. He was a Guest Editor for the Focus Issue on Microwave Photonics in *Optics Express* and Feature Issue on Microwave Photonics in *Photonics Research*, in 2013 and 2014, respectively. He is currently a Topical Editor for *Optics Letters*, and serves on the Editorial Board of the IEEE TRANSACTIONS ON MICROWAVE THEORY AND TECHNIQUES, *Optics Communications*, and *China Science Bulletin*. He is the Chair of numerous international conferences, symposia, and workshops, including the Vice Technical Program Committee (TPC) Chair of the *IEEE Microwave Photonics Conference* in 2007, the TPC Cochair of the *Asia-Pacific Microwave Photonics Conference*, in 2009 and 2010, the TPC Chair of the high-speed and broadband wireless technologies subcommittee of the *IEEE Radio Wireless Symposium* from 2009 to 2012, the TPC Chair of the microwave photonics subcommittee of the *IEEE Photonics Society Annual Meeting* in 2009, the TPC Chair of the *IEEE Microwave Photonics Conference* in 2010, the General Cochair of the *IEEE Microwave Photonics Conference* in 2011, the TPC Cochair of the *IEEE Microwave Photonics Conference* in 2014, and the General Cochair of the *IEEE Microwave Photonics Conference* in 2015. He received the International Creative Research Award at the University of Ottawa in 2005 and he also received the George S. Glinski Award for excellence in research in 2007. He was selected to receive an inaugural OSA Outstanding Reviewer Award in 2012.